

1 **Title:** The relationships between cochlear nerve health and AzBio sentence  
2 scores in quiet and noise in postlingually deafened adult cochlear implant  
3 users

4 **Authors:** Zi Gao<sup>1</sup>, PhD; Yi Yuan<sup>2</sup>, PhD; Jacob J. Oleson<sup>3</sup>, PhD; Christopher R.  
5 Mueller<sup>1</sup>; Ian C. Bruce<sup>4</sup>, PhD; René H. Gifford<sup>5</sup>, PhD; Shuman He<sup>1</sup>, MD,  
6 PhD

7 **Affiliations:** <sup>1</sup>Department of Otolaryngology – Head and Neck Surgery, The Ohio State  
8 University, Columbus, OH 43212  
9 <sup>2</sup>Department of Audiology, San José State University, San José, CA 95192  
10 <sup>3</sup>Department of Biostatistics, The University of Iowa, Iowa City, IA 52242  
11 <sup>4</sup>Department of Electrical and Computer Engineering, McMaster  
12 University, Hamilton, ON, L8S 4K1, Canada  
13 <sup>5</sup>Department of Hearing and Speech Sciences, Vanderbilt School of  
14 Medicine, Nashville, TN 37232

15 **Correspondence:** Shuman He, MD, PhD  
16 Eye and Ear Institute  
17 Department of Otolaryngology – Head and Neck Surgery  
18 The Ohio State University  
19 915 Olentangy River Road, Suite 4000  
20 Columbus, OH 43212  
21 Phone: 614-293-5963  
22 Fax: 614-293-7292  
23 Email: Shuman.He@osumc.edu

24 **Conflict of Interest:** None.

25 **Source of Funding:** This work was supported by grants from the National Institutes of Health

26 awarded to SH [grant numbers 1R01 DC016038 and R21 DC019458].

27 **Author Contributions:** ZG participated in data analysis, drafted and approved the final version

28 of this paper. YY participated in data collection, provided critical

29 comments, and approved the final version of this paper. JJO conducted

30 statistical analyses, provided critical comments, and approved the final

31 version of this paper. CRM participated in data collection and analysis,

32 provided critical comments, and approved the final version of this paper.

33 ICB and RHG provided critical comments and approved the final

34 version of this paper. SH designed this study, participated in data

35 analysis, provided critical comments, and approved the final version of

36 this paper.



60 **Results:** The correlation between the  $IPGE_{slope}$  and the PLV was negligible and not statistically  
61 significant. The PLV, but not the  $IPGE_{slope}$ , differed significantly across electrodes, where the  
62 apical electrodes had larger PLVs (better neural synchrony) than the basal electrodes. The  
63  $IPGE_{slope}$ , but not the PLV, was significantly correlated with participant's age, where smaller  
64  $IPGE_{slope}$  values (poorer CN health) were associated with more advanced age. The PLV, but not  
65 the  $IPGE_{slope}$ , was significantly associated with AzBio scores in noise, where larger PLVs  
66 predicted better speech perception in noise. Neither the PLV nor the  $IPGE_{slope}$  was significantly  
67 associated with AzBio score in quiet. The result patterns remained the same regardless of  
68 whether the mean values of the  $IPGE_{slope}$  and the PLV were weighted by the AzBio FIF.

69

70 **Conclusions:** The  $IPGE_{slope}$  and the PLV quantify different aspects of CN health. The positive  
71 association between the PLV and AzBio scores suggests that neural synchrony is important for  
72 speech perception in noise in adult CI users. The lack of association between age and the PLV  
73 indicates that reduced neural synchrony in the CN is unlikely the primary factor accounting for  
74 the greater deficits in understanding speech in noise observed in elderly, as compared to younger,  
75 CI users.

76

77 **Key words:** cochlear implants, cochlear nerve, neural synchrony, neural health, speech  
78 perception

79 **INTRODUCTION**

80 The cochlear implant (CI), a prosthesis that partially restores hearing through stimulating  
81 the cochlear nerve (CN) via electrodes surgically implanted into the inner ear, is a standard  
82 treatment option for listeners with sensorineural hearing loss (for a review, see Zeng 2004).  
83 Since electrical stimulation takes place at the auditory periphery, subsequent transmission of the  
84 signals by the CN is a prerequisite for the central auditory system's ability to access and process  
85 the sound information. Therefore, it is believed that the neural health of the CN is crucial for the  
86 success of CI treatment (e.g., He et al. 2017; Zamaninezhad et al. 2023). The association  
87 between the CN health and hearing performance in CI users has been supported by post-mortem  
88 observations, where within-subject between-ear comparisons showed that the ear with a larger  
89 amount of spiral ganglion neurons (SGNs) consistently yielded a better word recognition  
90 performance (Seyyedi et al. 2014). However, due to the invasiveness of the histological  
91 procedures, direct examination of the CN is not feasible in living human CI users. Rather, non-  
92 invasive electrophysiological measures, such as the electrically evoked compound action  
93 potential (eCAP), have been developed to assess the CN health status of human CI users in  
94 research and clinical settings.

95 The eCAP is a near-field recorded, synchronized response of a population of CN fibers  
96 elicited by electrically stimulating a CI electrode, which has been used to evaluate neural  
97 encoding of electrical stimulation at the CN, such as spectral resolution (Won et al. 2014), neural  
98 adaptation (Hughes et al. 2012; He et al. 2023), and amplitude modulation encoding (Tejani et al.  
99 2017) in CI users. Morphologically, a typical eCAP waveform consists of a negative peak (N1)  
100 at around 0.2-0.4 ms after stimulus onset, followed by a positive peak (P2) at around 0.6-0.8 ms  
101 after stimulus onset (e.g., Brown et al. 1990). The amplitude of the eCAP waveform is defined as

102 the difference in voltages between P2 and N1, and it increases with the stimulation level. The  
103 relationship between stimulation level and eCAP amplitude can be depicted using an amplitude  
104 growth function (AGF), also known as the input/output (I/O) function.

105 The slope of eCAP AGF has been shown to be associated with the density of SGNs in  
106 animal studies, where steeper slopes indicate higher SGN density in pharmaceutically deafened,  
107 implanted animals (Pfungst et al. 2015). Aligned with the animal results, shallower eCAP slopes  
108 were observed in pediatric CI users with CN deficiency (CND) compared to those with normal-  
109 sized CNs (He et al. 2018). However, since the raw eCAP responses are susceptible to inter-  
110 patient and inter-electrode differences in non-neural factors (Brochier et al. 2021), researchers  
111 have been seeking to overcome this drawback by using the differences between eCAP-derived  
112 measurements under various stimulation conditions to assess CN health. Animal studies have  
113 shown that the sensitivity of the eCAP amplitude to changes in the interphase gap (IPG) of  
114 biphasic, electrical pulses is correlated with SGN survival. Specifically, larger effects of IPG  
115 (IPG) on eCAP amplitude (Prado-Guitierrez et al. 2006) and the AGF slope (Ramekers et al.  
116 2014; Schwartz-Leyzac et al. 2019) are associated with higher SGN density in guinea pigs.  
117 Consistent with these results measured in animal models, children with normal-sized CNs  
118 showed larger IPG effects on the AGF slope ( $IPGE_{slope}$ ) than children with cochlear congenital  
119 CND (Yuan et al. 2022). In addition, the  $IPGE_{slope}$  has been shown to be positively correlated  
120 with sentence and consonant recognition (Schwartz-Leyzac & Pfungst 2018) and speech reception  
121 threshold (SRT; Zamaninezhad et al. 2023) in postlingually deafened adult CI users. Brochier et  
122 al. (2021) reanalyzed data from previous animal (Prado-Guitierrez et al. 2006) and human  
123 (McKay & Smale 2017) studies and proposed based on computational modeling results that IPG  
124 effect on stimulation level offset ( $IPGE_{offset}$ ) outperformed the  $IPGE_{slope}$  in controlling for non-

125 neural factors, yet Zamaninezhad et al. (2023) failed to establish an association between the  
126  $IPGE_{\text{offset}}$  and speech perception measurements in CI users. In a recent computational modeling  
127 study, Takanen et al. (2024) demonstrated that the  $IPGE_{\text{slope}}$  calculated as the absolute difference  
128 between the AGF slopes on a linear I/O scale is dependent on neural survival, and that non-  
129 neural factors had little interference on the  $IPGE_{\text{slope}}$ . Taken together, despite some discrepancies,  
130 evidence from animal, human and computational research are converging in suggesting that the  
131  $IPGE_{\text{slope}}$  is an indicator of CN survival.

132         While having sufficient CN fibers responding to auditory input is a prerequisite for  
133 auditory perception, CN density alone does not guarantee good hearing functions in challenging  
134 listening environments. In theory, effective and accurate representation of sound signals that  
135 allows the listener to separate target signals from noise requires synchronous firing across  
136 neurons, which in turn depends on the health status of the CN, as demonstrated in animal and  
137 computational modeling studies (Kim et al. 2013; Heshmat et al. 2020). Neural  
138 desynchronization leads to a smeared representation of temporal cues, so that even though the  
139 ability to detect sound in quiet may be minimally affected, hearing performance in noise would  
140 degrade drastically. This scenario is exemplified by some listeners with auditory neuropathy  
141 spectrum disorder (ANSD), who have normal or relatively good behavioral audiometric  
142 thresholds and speech perception in quiet, but disproportionately impaired signal detection and  
143 speech perception in noise (Kraus et al. 2000; Zeng et al. 2005). The electrophysiological  
144 measures of patients with ANSD are characterized by a relatively normal cochlear microphonic  
145 and/or otoacoustic emission (OAE) response, and an abnormal or absent auditory brainstem  
146 response (ABR), which has been interpreted as a lack of synchrony across CN fibers despite a  
147 relatively normal hair cell function (e.g., Starr et al. 2008). The crucial role of neural synchrony

148 in acoustic hearing has been further supported by the compound action potential (CAP) recorded  
149 in normal hearing (NH) listeners, where the level of neural synchrony, quantified with the phase  
150 locking value (PLV) of trial-by-trial CAP measurements, was found to be a strong predictor of  
151 recognition scores for speech in noise and time-compressed speech in quiet (Harris et al. 2021).

152 Due to the difference between acoustic and electrical hearing, the observations in  
153 listeners with NH or ANSD may not be readily generalizable to CI users. For many CI users,  
154 speech perception in noise is a challenging task despite excellent hearing performance in quiet  
155 (Zaltz et al. 2020). Histological observations of SGN dystrophy and demyelination in listeners  
156 with various hearing profiles (Nadol 1997; Wu et al. 2019) suggest that reduced neural  
157 synchrony could be an underlying cause of poor speech perception in noise in CI users.  
158 However, this proposed relationship has rarely been evaluated, largely due to the lack of  
159 electrophysiological measures of neural synchrony of the CN. We recently developed a new  
160 method to quantify peripheral neural synchrony in CI users, where the PLV of trial-by-trial  
161 eCAP responses was used as an index to quantify the degree of neural synchrony in the  
162 responses generated by CN fibers across multiple electrical stimulations (He et al. 2024). We  
163 demonstrated that higher PLVs are associated with better temporal resolution and smaller effects  
164 of noise on word recognition in post-lingually deafened adult CI users, consistent with the  
165 hypothesized effect of neural synchrony on hearing performance in electrical hearing.

166 In summary, previous research has established both CN survival and neural synchrony as  
167 crucial factors contributing to hearing performance in CI users. However, considering that nerve  
168 damage can result in both lower neural density and poorer synchronization, as has been shown in  
169 computational models (Heshmat et al. 2020), little is known about whether the contributions of  
170 neural survival and synchrony to hearing performance are independent or overlapping.



171 Observations in NH listeners by Harris et al. (2021) suggest that neural engagement and  
172 synchrony are two separate dimensions that vary differently with changes in stimulus level. In  
173 human CI users, the number and synchrony of excited CN fibers have been modeled using  
174 retrospective deconvolution performed on intraoperative eCAP recordings, both significantly  
175 associated with postoperative speech recognition scores (Dong et al. 2023). However, the model  
176 was built upon assumptions about the shape of unitary response from CN fibers, which have not  
177 been directly validated in humans (Dong et al. 2020; Dong et al. 2023). While the  $IPGE_{slope}$  and  
178 the PLV in CI users have been measured postoperatively in separate experimental studies to  
179 assess their association with speech perception (Schvartz-Leyzac & Pfingst 2018; Zamaninezhad  
180 et al. 2023; He et al. 2024), it is unclear whether the biological underpinnings of these two  
181 indices are orthogonal and impact speech perception differently depending on listening  
182 conditions.

183 To address this critical knowledge gap, we measured the  $IPGE_{slope}$ , the PLV and speech  
184 perception in the same group of postlingually deafened adult CI users and evaluated their  
185 relationships. Speech perception was measured using AzBio sentences (Spahr et al. 2012), a  
186 speech corpus consisting of multiple lists of everyday sentences with similar levels of difficulty.  
187 Based on previous studies on the effects of neural survival and neural synchrony on speech  
188 perception in listeners with various hearing profiles, we hypothesized that (1) the  $IPGE_{slope}$  and  
189 the PLV are two independent measures of CN health (Harris et al. 2021; Kraus et al. 2000); (2)  
190 the  $IPGE_{slope}$  is positively associated with speech perception in quiet (Zamaninezhad et al. 2023);  
191 (3) the PLV is positively associated with speech perception in noise (Zeng et al. 2005; Harris et  
192 al. 2021; He et al. 2024).

193

194  
195  
196  
197  
198  
199  
200  
201  
202  
203  
204  
205  
206  
207  
208  
209  
210  
211  
212

## MATERIALS AND METHODS

### Participants

Study participants included 24 postlingually deafened CI users (age range: 36.79-84.04 years, mean = 63.69 yrs, standard deviation  $SD = 11.83$  yrs; 12 female, 12 male). Twenty of them also participated in our previous study on the development and validation of the eCAP PLV measurement (He et al. 2024), and their PLV data were reused in the current study. All participants were native speakers of American English and used a Cochlear® Nucleus™ device (Cochlear Ltd., New South Wales, Australia) in the test ear for at least two years prior to this study. All participants had a full 22-electrode insertion with their devices, as confirmed by postoperative computerized tomography scans. Only one ear was tested in each participant. None of the participants had any functional acoustic hearing in either ear. All participants achieved a score of 26 or above on the Montreal Cognitive Assessment (Nasreddine et al. 2005). Demographic information and hearing loss etiology of the participants are listed in Table 1. All participants provided written informed consent at their initial visit to the lab prior to data collection and were compensated for their time. The study was approved by the Biomedical Institutional Review Board at the Ohio State University (No. 2017H0131).

Table 1. Demographic information of all participants. The participant IDs are not known to anyone outside the research group, including the participants themselves.

Participant ID	Ear tested	Age range at testing (yrs)	Internal device and electrode array	Hearing loss etiology	Electrodes tested
S01	L	61-65	CI 512	Sudden SNHL	3, 9, 14, 20
S02	L	66-70	CI 512	Meniere's disease	3, 9, 15, 18
S03	R	66-70	CI 24RE(CA)	Unknown	3, 9, 15, 21
S04	L	56-60	CI 24RE(CA)	Head Trauma	3, 9, 15, 21

S05	R	61-65	CI 24RE(CA)	Unknown	8, 12, 15, 18
S06	L	51-55	CI 532	Unknown	4, 9, 15, 21
S07	R	61-65	CI 522	Head Trauma	6, 9, 18, 20
S08	R	36-40	CI 24RE(CA)	Unknown	3, 9, 15, 21
S09	R	56-60	CI 24RE(CA)	Unknown	3, 9, 15, 21
S10	R	61-65	CI 532	Unknown	3, 9, 15, 21
S11	R	66-70	CI 532	Unknown	3, 9, 15, 21
S12	L	76-80	CI 422	Unknown	4, 9, 15, 21
S13	L	61-65	CI 632	Unknown	3, 9, 15, 21
S14	R	66-70	CI 24RE(CA)	Unknown	3, 15, 21
S15	L	66-70	CI 532	Vestibular Schwannoma	3, 9, 15, 21
S16	R	81-85	CI 532	Unknown	3, 7, 10, 17
S17	L	71-75	CI 622	Unknown	6, 9, 15, 21
S18	R	81-85	CI 632	Unknown	3, 9, 15, 21
S19	R	51-55	CI 632	Unknown	3, 9, 15, 21
S20	L	56-60	CI 632	Unknown	3, 15, 18
S21	L	56-60	CI 532	Usher	3, 9, 15, 21
S22	L	76-80	CI 632	Unknown	3, 9, 15, 21
S23	L	41-45	CI 612	Vestibular Schwannoma	6, 15, 21
S24	L	51-55	CI 612	Unknown	5, 9, 15, 21

213

## 214 **Stimuli and Apparatus**

215 For eCAP recordings, the stimulus was a charge-balanced, cathodic leading biphasic  
216 pulse with a pulse-phase duration of 25  $\mu$ s. The IPG between the cathodic and anodic phases, as  
217 well as the presentation levels, varied across measurements, as detailed in the “Procedures”  
218 section. All eCAP recordings were performed using the neural response telemetry function  
219 implemented in the Custom Sound EP software v6.0 (Cochlear Ltd., New South Wales,  
220 Australia).

221 For speech perception tests, the stimuli were meaningful sentences (e.g., “The vacation  
222 was cancelled on account of weather.”) from the AzBio sentence corpus (Spahr et al. 2012),  
223 recorded by two female and two male native American English speakers. The sentences  
224 presented to each participant and for each condition were evenly distributed across the four

225 speakers. The background noise was a ten-talker babble presented at two signal-to-noise ratios  
226 (SNRs): +10 dB and +5 dB. All stimuli were delivered via a loudspeaker (RadioEar Corporation,  
227 PA) placed 1 m in front of the participant at 0° azimuth in a sound-attenuated booth.

228

## 229 **Procedures**

### 230 *Testing electrodes*

231 The default testing sites for eCAP measurements were electrodes 3, 9, 15, and 21 (i.e., e3,  
232 e9, e15 and e21). These electrodes were selected to cover a wide range along the array with  
233 relatively equal numerical separations in between, while keeping the testing time reasonable. In  
234 the case of an open- or short-circuit at a default electrode, a nearby alternative electrode was  
235 tested. Three participants (S14, S20, and S23) were tested at only three electrodes due to time  
236 constraints. The electrodes tested for each participant can be found in Table 1.

237

### 238 *Behavioral C Level Measures*

239 The maximum comfortable level (C level) for eCAP stimuli at each IPG level (7  $\mu$ s and  
240 42  $\mu$ s) was determined via subjective rating using an ascending procedure. Prior to the  
241 measurement, participants were shown a visual scale of 1 (“barely audible”) to 10 (“very  
242 uncomfortable”) and were instructed to give a loudness rating using verbal responses or hand  
243 gestures following each stimulus presentation. Each presentation consisted of five pulses  
244 delivered at a probe rate of 15 Hz. The stimuli were first presented at a relatively low level and  
245 gradually increased in steps of 3-5 clinical levels (CLs) until a rating of “7” was reached, then in  
246 steps of 1-2 CLs until a rating of “8” was reached. The lowest level that corresponds to a rating  
247 of “8” (“maximal comfort”) was recorded as the behavioral C level.

248

249 *eCAP Measures*

250         The eCAP was measured using a two-pulse, forward-masking paradigm (Brown et al.,  
251 1990), where the masker pulse was always presented at 10 CLs higher than the probe pulse. The  
252 masker pulses were delivered at the testing electrode, and the eCAP responses were recorded two  
253 electrodes away from the testing electrode in the apical direction. There was an exception for  
254 electrode 21, which was recorded two electrodes away in the basal direction (i.e., electrode 19).  
255 The probe pulses were presented at a probe rate of 15 Hz with a masker-probe interval of 400  $\mu$ s.  
256 The total number of trials in each stimulation sequence differed across measurements, as detailed  
257 below. Responses were recorded at a sampling rate of 20,492 Hz with a sampling delay of 122  
258  $\mu$ s, an amplifier gain of 50 dB, and a monopolar-coupled stimulation mode.

259

260 *Measure of Neural Survival: the  $IPGE_{slope}$*

261         In this study, the  $IPGE_{slope}$  was operationally defined as the absolute difference (in  
262 mV/dB) between the AGF slopes with IPGs of 42  $\mu$ s and 7  $\mu$ s, and therefore, its measurement  
263 involved acquiring an AGF and calculating its slope at each IPG level for each participant. For  
264 both IPG levels, the maximum presentation level of the stimuli was the behavioral C level  
265 measured with an IPG of 42  $\mu$ s. To acquire AGFs, the eCAP measurement started at the  
266 maximum presentation level and decreased in steps of 1 CL for five steps, then in steps of 5 CUs  
267 until no peaks could be visually identified in the eCAP waveform, i.e., when the threshold is  
268 reached. Additional presentation levels in steps of 1 CL for five steps near and above the eCAP  
269 threshold were tested. At each presentation level, the eCAP waveform was acquired by  
270 averaging the raw responses to 50 pulses. The visual identification of eCAP peaks, or lack

271 thereof, was performed by the experimenter at the time of testing and rechecked by an expert  
272 researcher (author S.H.) offline. The AGF slope at each IPG level was calculated using the  
273 window method developed by Skidmore et al. (2022), where linear regressions were performed  
274 on sliding windows along a resampled AGF, and the largest slope among all windows was  
275 regarded as the AGF slope. All calculations were performed using MATLAB 2021b  
276 (MathWorks, MA).

277

### 278 *Measure of Neural Synchrony: the PLV*

279 For each participant and electrode, the PLV was derived from 400 eCAP trials measured  
280 using biphasic pulses with an IPG of 7  $\mu$ s presented at the behavioral C level, using the method  
281 developed by He et al. (2024). The PLV is a unitless value between 0 and 1, where 0 means that  
282 the phases were randomly distributed across trials, and 1 means that the phases were perfectly  
283 correlated. To calculate the PLV, the eCAP responses were time-frequency decomposed at six  
284 linearly spaced frequencies (788.2, 1576.3, 2364.4, 3152.6, 3941.0, and 4729.2 Hz) and divided  
285 into six partially overlapped time frames with an onset-to-onset interval of 48.8  $\mu$ s and a length  
286 of 1561.6  $\mu$ s. At each frequency and within each time frame, the unit vectors representing the  
287 phases of the 400 individual trials were averaged, and the length of the averaged vector was  
288 taken as the time-frequency-specific PLV. The formula for calculating the PLV at the time  $t$  and  
289 the frequency  $f$  based on  $N$  individual trials is:

290

$$PLV(f, t) = \left| \frac{1}{N} \sum_{k=1}^N \frac{F_k(f, t)}{|F_k(f, t)|} \right|$$

291 The PLV of the electrode was then obtained by averaging all time-frequency-specific PLVs  
292 calculated from the eCAP responses at that electrode. The time-frequency decomposition and the

293 calculation of the PLV were performed using MATLAB R2021b and the newtimef.m function  
294 from EEGLAB v2022.1 (Delorme & Makeig 2004).

295

### 296 *Measure of Speech Perception: AzBio Scores*

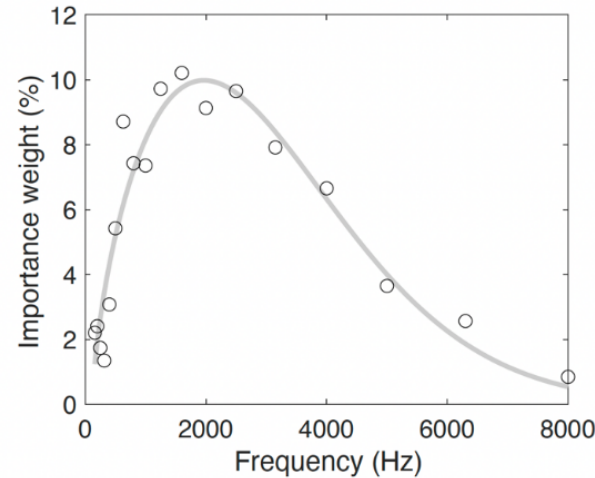
297 Each participant was tested with AzBio sentences (Spahr et al. 2012) under three  
298 conditions: in quiet and in a ten-talker babble background noise with SNRs of +10 and +5 dB,  
299 respectively. The sentences were presented at 60 dB SPL in all conditions. For each participant  
300 and condition, a sentence list was randomly selected from Lists 1-8 of the AzBio corpus, each  
301 consisting of 20 sentences. For each participant, different word lists were used for different  
302 conditions. Participants were instructed to repeat back after each sentence and were encouraged  
303 to guess if they were unsure about what they heard. An experimenter recorded the number of  
304 words they correctly repeated in each sentence. The AzBio score was calculated as the number of  
305 words in the list correctly repeated by the participant, divided by the total number of words in the  
306 list. All words in the list, including prepositions, counted towards the score.

307

### 308 *Averaging $IPGE_{slope}$ and PLV Values across Electrodes*

309 For each participant, the values of the  $IPGE_{slope}$  and the PLV were averaged across all  
310 tested electrodes as an overall representation of CN health across the cochlea. Both weighted and  
311 unweighted averages were calculated for both parameters. To calculate the weighted average, the  
312 results were weighted based on the frequency importance function (FIF) derived from AzBio  
313 scores under various spectral filtering conditions and SNRs in NH listeners (Lee & Mendel  
314 2017). The FIF was fitted to a four-parameter Weibull function in SigmaPlot v15 (Grafiti LLC,  
315 CA). For each participant, the importance weight of each test electrode was calculated using the

316 fitted Weibull function based on the electrode's central frequency derived from the frequency-to-  
317 electrode table of the participant's everyday programming map. The individual values of the  
318 empirically measured AzBio FIF and the fitted curve are shown in Figure 1. The unweighted  
319 average was calculated as the arithmetic means of the  $IPGE_{slope}$  and the PLV values across all  
320 tested electrodes for each participant.



321  
322 Figure 1. Individual AzBio FIF values (black circles) measured by Lee and Mendel (2017) and  
323 the fitted Weibull function (gray line)

324

## 325 Data Analysis

326 The  $IPGE_{slope}$  and PLV values were compared across electrodes using linear mixed-effect  
327 models. Pairwise comparisons between the electrodes were performed using the Tukey method  
328 for  $p$ -value adjustment. The pairwise relationships between the  $IPGE_{slope}$ , the PLV, and age at  
329 testing were assessed using either Pearson or Spearman correlation tests for variable pairs  
330 depending on the results of the Shapiro-Wilk normality test. Multiple linear regressions with  
331 AzBio score as the outcome and the  $IPGE_{slope}$  and the PLV as predictors were performed to  
332 evaluate the associations among the three variables under each testing condition (quiet, +10 dB,



333 and +5 dB SNR). Participant's age was added to the regression models as a covariate to control  
334 for the potential effects of advanced age on speech perception and/or eCAP measurements, as  
335 have been demonstrated in CI users (Roberts et al. 2013; Sladen & Zappler 2015; Xie et al. 2019;  
336 Jahn & Arenberg 2020). If the residuals were not approximately normally distributed, the  
337 outcome variables were transformed with appropriate methods to ensure that the normal residual  
338 assumption of linear regression is met. Correlation tests were performed in JASP v0.18.3 (JASP  
339 Team 2024), and the regressions were performed in R v4.4.1 (R Core Team 2024), with the lme4  
340 (Bates et al. 2015), emmeans (Lenth 2024), and lmerTest (Kuznetsova et al. 2017) packages used  
341 for the linear mixed-effect models.

342

343

## RESULTS

344

345

346

347

348

349

350

351

352

353

354

355

The individual  $IPGE_{slope}$  and PLV values measured at each electrode are shown in Figure 2, with the range, mean, and standard deviation (SD) listed in Table 2. To assess the potential differences in the two measurements across electrodes, two linear mixed-effect regressions were performed with the  $IPGE_{slope}$  and the PLV as the outcome variables, the electrode category as the fixed effect, and participant as the random effect. The electrode categories correspond to the four default testing locations: e3, e9, e15, and e21. If other electrodes were measured in lieu of the default electrodes, they were assigned to one of the categories based on their locations relative to the other electrodes tested in the same participant. For example, among the four electrodes tested in participant S05, e8 was the most basal electrode and therefore categorized as “e3” in the regression model. The category “e3” was used as the reference level in the regressions. The degrees of freedom were estimated using the Satterthwaite's method. The results reveal an overall effect for PLV across electrodes ( $F_{(3, 66.2)} = 3.86, p = .013$ ). Focusing on

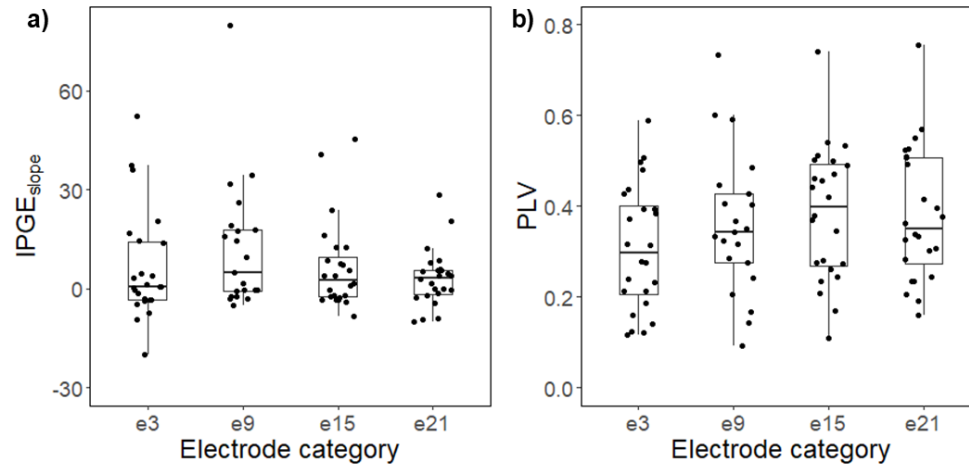
356 the pairwise comparisons, only two comparisons showed a statistically significant difference in  
357 PLVs which were e3 compared with the PLVs measured at e15 ( $t_{(66.0)} = 2.99, p = .020$ ) and e21  
358 ( $t_{(66.0)} = 2.88, p = .027$ ). The other comparisons were not significantly different which were e3  
359 with e9 ( $t_{(66.4)} = 1.64, p = .364$ ), e9 with e15 ( $t_{(66.4)} = 1.22, p = .615$ ), e9 with e21 ( $t_{(66.4)} = 1.12, p$   
360  $= .682$ ), and e15 with e21 ( $t_{(66.0)} = 0.11, p = .999$ ). The  $IPGE_{slope}$  did not significantly differ  
361 across electrodes ( $F_{(3, 66.6)} = 2.50, p = .067$ ). In the subsequent sections, the  $IPGE_{slope}$  and the  
362 PLV refer to the weighted averages of the corresponding values across electrodes for individual  
363 participants unless otherwise stated.

364

365 Table 2. Descriptive statistics of the  $IPGE_{slope}$  and the PLV values measured at different  
366 electrode locations. Values in each cell are listed in the format of “range, mean (SD)”.

<b>Electrode category</b>	<b>e3</b>	<b>e9</b>	<b>e15</b>	<b>e21</b>
PLV	0.117-0.590 0.309 (0.139)	0.092-0.734 0.342 (0.153)	0.109-0.741 0.384 (0.147)	0.160-0.755 0.381 (0.147)
$IPGE_{slope}$	-20.003-52.412 6.221 (16.515)	-4.982-79.901 12.152 (19.723)	-8.306-45.231 6.604 (13.486)	-10.068-28.455 3.203 (8.725)

367



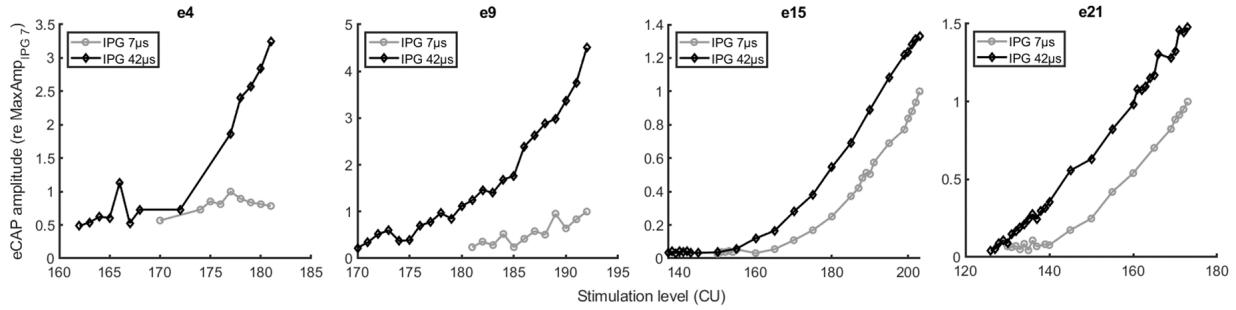
368

369 Figure 2. Individual values of (a) the IPGE<sub>slope</sub> and (b) the PLV by electrode category, which is  
370 named after the default electrodes. Values measured at non-default electrodes were categorized  
371 based on their locations relative to the other electrodes tested in the same participant. Boxes  
372 show the range between the first and the third quartile of the data values. The horizontal bars  
373 inside the boxes represent the median. The vertical whiskers show the range of values that are  
374 within 1.5 interquartile range (IQR) from the boxes.

375

### 376 **Correlations between the IPGE<sub>slope</sub>, the PLV, and age**

377 The eCAP AGFs acquired at different IPG durations from one example participant (S06)  
378 are shown in Figure 3. Time-frequency specific PLV values of the same participant are  
379 illustrated in Figure 4. Figure 5 shows the IPGE<sub>slope</sub> and PLV values of individual participants  
380 (panel a), along with their age (panels b-c). The values of the PLV were relatively uniformly  
381 distributed, while one outlier (S08) for the IPGE<sub>slope</sub> was identified both through visual  
382 inspection and descriptive statistics ( $>2$  SDs away from the mean). Spearman correlation tests  
383 showed that the IPGE<sub>slope</sub> and the PLV were not significantly correlated, either before ( $\rho_{(22)} =$   
384  $0.217, p = .308$ ) or after ( $\rho_{(21)} = 0.206, p = .345$ ) removing the outlier.



385

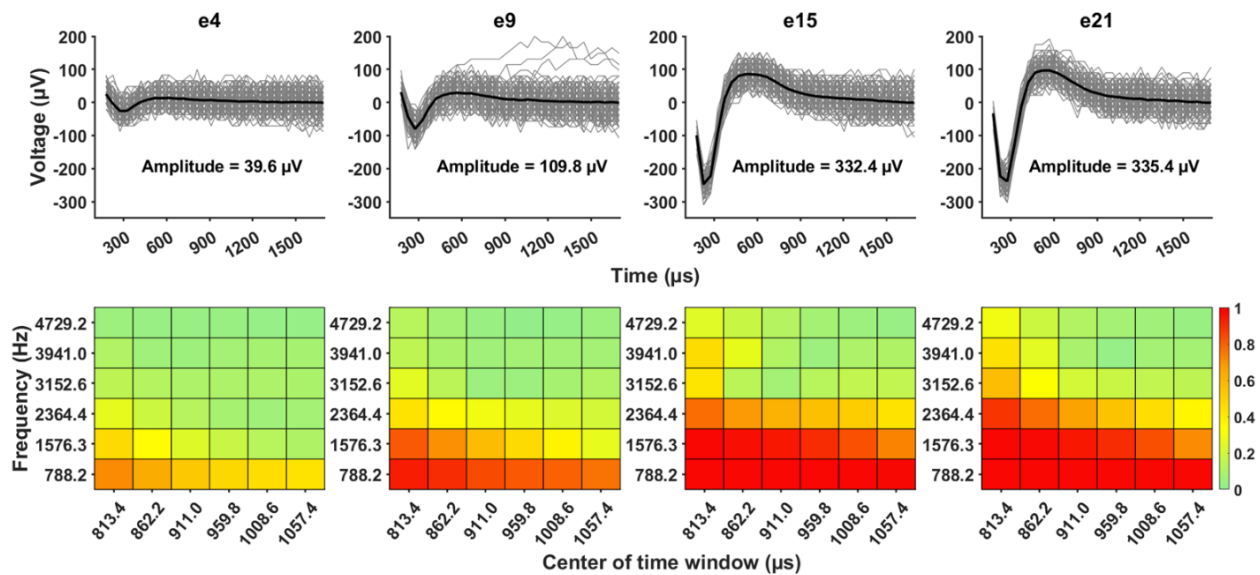
386 Figure 3. The AGFs measured with IPGs of 7  $\mu$ s and 42  $\mu$ s in one participant (S06), where the  
387 maximum stimulation level was set to the C level measured with a 42- $\mu$ s IPG at each electrode.

388 The amplitudes were normalized by dividing the maximum amplitude among the trials with a 7-

389  $\mu$ s IPG. Please note that the ranges of the axes are different across panels due to large

390 variabilities in eCAP thresholds, C-levels, and amplitudes across electrodes.

391



392

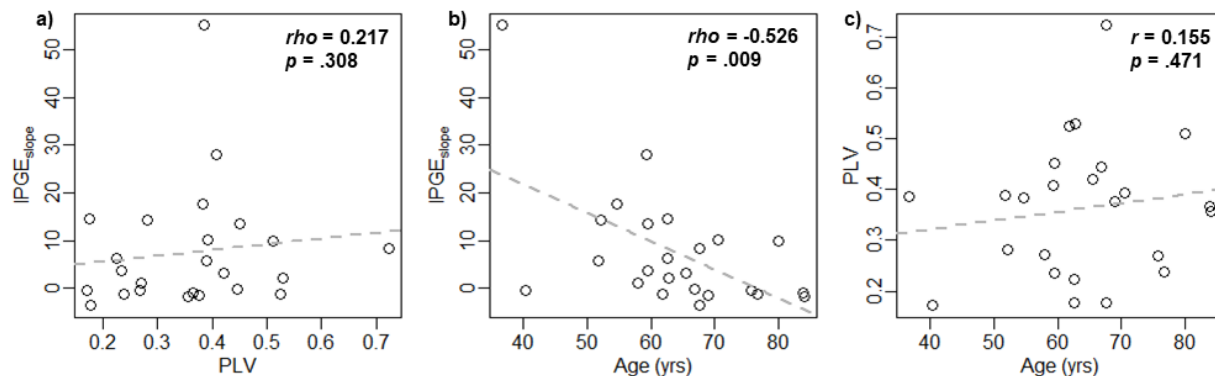
393 Figure 4. PLV values measured in one participant (S06). The time-frequency specific PLV

394 values are shown in the heatmaps. Bolded black lines represent eCAP responses averaged across

395 400 trials. Responses in individual trials are plotted with gray lines.

396

397 Although not a focus of this study, we assessed the relationships between age and the two  
398 CN health measures. Spearman correlation test results revealed a significant negative correlation  
399 between the  $IPGE_{slope}$  and age both before ( $\rho_{(22)} = -0.526, p = .009$ ) and after removing the  
400 outlier ( $\rho_{(21)} = -0.461, p = .028$ ). Pearson correlation test results showed that PLV was not  
401 significantly correlated with age, either before ( $r_{(22)} = 0.155, p = .471$ ) or after ( $r_{(21)} = 0.197, p$   
402  $= .369$ ) removing the outlier.



403  
404 Figure 5. Correlations between (a) the  $IPGE_{slope}$  and the PLV, (b) the  $IPGE_{slope}$  and age, and (c)  
405 the PLV and age. Data from all 24 participants were included in the figures. Each symbol  
406 indicates the result measured in one participant. The results of correlation tests are shown in each  
407 panel.

408  
409 The results reported in the subsequent sections were acquired from the full dataset  
410 without removing any outliers. It is worth noting that removing the  $IPGE_{slope}$  outlier did not  
411 change the pattern or statistical significance of the linear regression results.

412

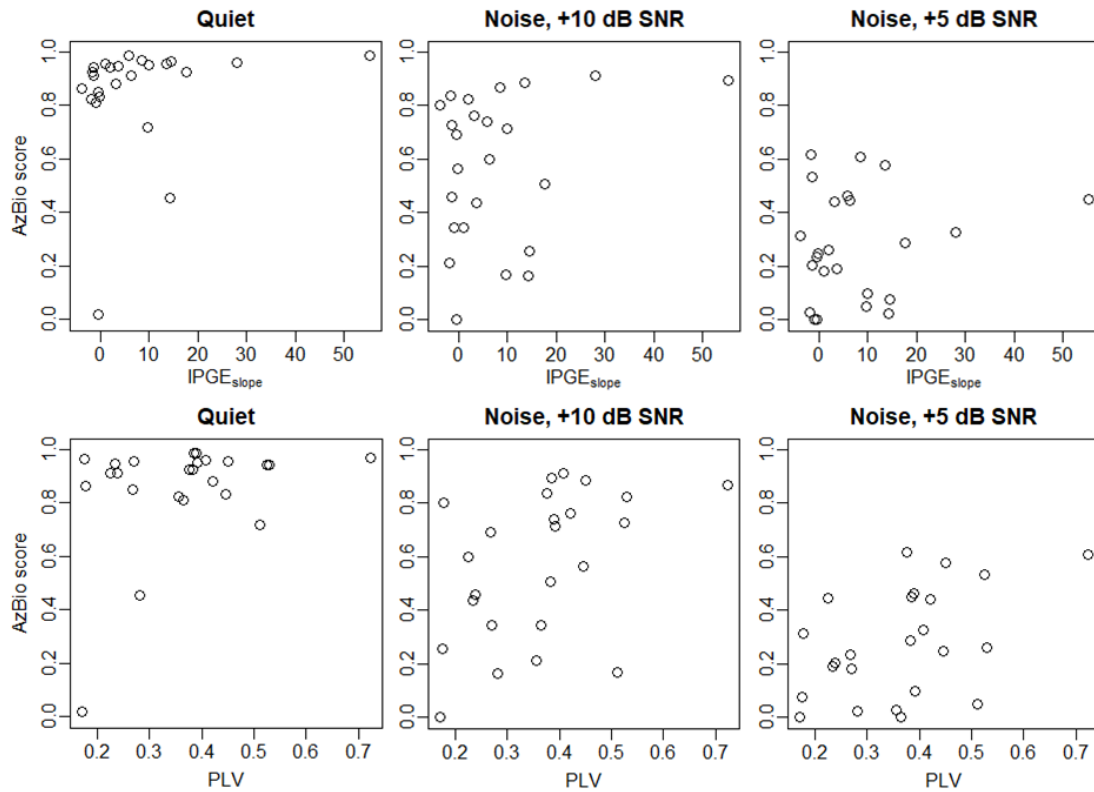
413 **The associations among the IPGE<sub>slope</sub>, the PLV and Speech Perception Scores**

414 The AzBio scores in quiet and noise are plotted against either the IPGE<sub>slope</sub> or the PLV in  
 415 Figure 6. The AzBio scores in quiet were rank transformed (i.e., the lowest and highest scores  
 416 were transformed into 1 and 24, respectively) due to non-normally distributed residuals when the  
 417 raw scores were used in the linear regression model (not reported here). The results of linear  
 418 regressions revealed significant associations between the PLV and AzBio scores in the two noise  
 419 conditions (+10 dB SNR:  $t_{(20)} = 2.19, p = .041$ ; +5 dB SNR:  $t_{(20)} = 2.70, p = .014$ ) after adjusting  
 420 for IPGE<sub>slope</sub> and age, where larger PLVs (better neural synchrony) are associated with higher  
 421 AzBio scores, but not in the quiet condition ( $t_{(20)} = 1.36, p = .190$ ). No significant association  
 422 between the IPGE<sub>slope</sub> and AzBio scores was observed in any testing conditions ( $p > .10$  in all  
 423 cases) after adjusting for PLV and age. Detailed results of the linear regression models are  
 424 available in Table 3. It is worth noting that rank-transformation of the AzBio scores in quiet did  
 425 not change the pattern or statistical significance of the results.

426  
 427 Table 3. Results of linear models examining the relationships between the IPGE<sub>slope</sub>, the PLV,  
 428 and AzBio scores measured in quiet and in two noise conditions. The AzBio scores in the quiet  
 429 condition were rank transformed to meet the normal residual assumption of linear regression.

Listening condition	Predictor	$\beta$ (SE)	$t$	$p$	Multiple $R^2$
Quiet	IPGE <sub>slope</sub>	0.1740 (0.1283)	1.355	.1905	0.3024
	PLV	14.0475 (10.3499)	1.357	.1899	
	age	-0.1348 (0.1394)	-0.967	.3451	
Noise, +10 dB SNR	IPGE <sub>slope</sub>	0.0037 (0.0052)	0.708	.4870	0.2526
	PLV	0.9120 (0.4164)	2.190	.0405*	
	age	-0.0015 (0.0056)	-0.269	.7910	
Noise, +5 dB SNR	IPGE <sub>slope</sub>	-0.0016 (0.0036)	-0.451	.6570	0.3050
	PLV	0.7951 (0.2943)	2.702	.0137*	
	age	-0.0061 (0.0040)	-1.550	.1367	

430



431

432 Figure 6. AzBio scores measured in quiet and in noise with +10 and +5 dB SNRs, plotted against  
433 the IPGE<sub>slope</sub> (top panels) and the PLV (bottom panels). Each symbol represents the AzBio score  
434 measured in one participant.

435

### 436 Electrode Weighting by AzBio FIF

437 To qualitatively evaluate whether weighting the IPGE<sub>slope</sub> and the PLV by the AzBio FIF  
438 modifies their relationships with AzBio scores, in a separate set of linear regressions, we used  
439 unweighted averages of the IPGE<sub>slope</sub> and the PLV in lieu of their weighted counterparts. Overall,  
440 the result patterns and statistical significance remained the same in the unweighted version of the  
441 linear regressions, where the relationships between the PLV and AzBio scores were statistically  
442 significant in the two noise conditions (+10 dB SNR:  $t_{(20)} = 2.29, p = .033$ ; +5 dB SNR:  $t_{(20)} =$   
443  $2.75, p = .012$ ) but not in the quiet condition ( $t_{(20)} = 1.08, p = .292$ ), and no significant

444 relationship between the  $IPGE_{slope}$  and AzBio scores was observed in any of the tested conditions  
445 ( $p > .10$  in all cases).

446

447

## DISCUSSION

448 This study assessed the relationships between two CN health measures, the  $IPGE_{slope}$  and  
449 the PLV, and evaluated their contributions to speech perception in quiet and noise in  
450 postlingually deafened adult CI users. We hypothesized that the  $IPGE_{slope}$  and the PLV are two  
451 independent measures predictive of speech recognition scores in quiet and in noise, respectively.  
452 The hypotheses were partially supported by the results showing that the correlation between the  
453  $IPGE_{slope}$  and the PLV was non-significant and negligible, and that the speech perception scores  
454 measured in noise were positively associated with the PLV. However, contrary to our hypothesis,  
455 we did not observe significant associations between the  $IPGE_{slope}$  and speech perception  
456 measured either in quiet or in noise.

457

### Peripheral Neural Survival and Synchrony

459 The lack of correlation between the  $IPGE_{slope}$  and the PLV suggests that they are  
460 measuring different aspects of CN health. The result is consistent with the previously  
461 documented partial dissociation between neural survival and synchrony in patients with ANSD  
462 due to perinatal oxygen deprivation, where magnetic resonance imaging showed no white matter  
463 abnormalities in the auditory system compared to NH controls (Zanin & Rance 2024). These  
464 observations are aligned with the physiological process of neural deterioration: damages of the  
465 neuronal structure such as axonal dystrophy and demyelination progress at different rates across  
466 neurons (Leake & Hradek 1988), resulting in reduced level of firing synchrony across neurons



467 even without significant reduction in the number of surviving neurons (Resnick et al. 2018). The  
468 deterioration of the bipolar SGNs starts at the peripheral axon, which connects the SGN soma to  
469 the organ of Corti in the cochlea (Xing et al. 2012). Even after the complete loss of the peripheral  
470 axon, the soma and the central axon of the SGN (i.e., unipolar SGN) can survive for decades  
471 (Rask-Andersen et al. 2010), and the proportion of unipolar SGNs increases steadily with age  
472 (Wu et al. 2023). This process gives rise to a key difference between acoustic and electric  
473 hearing. While the loss of peripheral SGN axons likely contributes to impairment in acoustic  
474 hearing (Wu et al. 2019; Wu et al. 2020; Wu et al. 2021), electric hearing can be achieved even  
475 without the peripheral axons, as the stimulation can directly reach the somata and/or the central  
476 axons of SGNs (Javel & Shepherd 2000). Such differences in the initiation sites of CN action  
477 potentials in electric, as compared to acoustic, hearing could further increase the variabilities in  
478 neural synchrony among CI users, which may not be captured by measures of SGN survival such  
479 as the  $IPGE_{slope}$ .

480         The dissociation between the  $IPGE_{slope}$  and the PLV was also corroborated by the  
481 observations on their different variabilities across electrodes and age. The PLV, but not the  
482  $IPGE_{slope}$ , was significantly different across electrodes, showing better neural synchrony at the  
483 apical than the basal locations along the electrode array. This result is consistent with the typical  
484 pattern of hearing impairment, which starts with the basal locations (higher frequencies) and  
485 gradually extends in the apical direction (Huang & Tang 2010; Wu et al. 2020; Wu et al. 2023).  
486 In addition, the lack of difference across electrodes in the  $IPGE_{slope}$  indicates that the gradient of  
487 hearing impairment across frequencies may be a result of varied degrees of damage in the  
488 peripheral axons, rather than in the count of SGN somata, at least in CI users. The negative  
489 association between the  $IPGE_{slope}$  and listener's age suggests poorer neural survival in elders as

490 compared to younger listeners, which is consistent with the trend observed in a recent post-  
491 mortem temporal bone study in listeners with acoustic hearing (Wu et al. 2023). Interestingly,  
492 the PLV was not significantly correlated with age, indicating that reduced neural synchrony may  
493 not be the primary factor accounting for the age-related deterioration in speech-in-noise  
494 perception, at least in CI users. This observation challenges the hypothesized role of neural  
495 synchrony in age-related hearing loss (e.g., Rumschlag et al. 2022). Further research is warranted  
496 to compare the PLVs across listeners from a wider range of age groups and with various hearing-  
497 loss etiologies to fully investigate the role of neural synchrony, or lack thereof, in age-related  
498 hearing deterioration in CI users.

499

#### 500 **Peripheral Neural Synchrony Contributes to Speech Perception in Noise**

501 We observed significant positive associations between the PLV and AzBio scores  
502 measured in noise, and a similar trend in the quiet condition that slightly missed significance,  
503 suggesting that neural synchrony is important for speech perception particularly in the presence  
504 of background noise. These results are consistent with the data from our previous study on CI  
505 users (He et al. 2024). This observation also agrees with and expands the findings by Harris et al.  
506 (2021), where the CAP-derived PLV was shown to be a strong predictor of the perception of  
507 time-compressed speech and speech in noise in NH listeners. These results highlight the  
508 importance of neural synchrony of the CN in speech perception in listeners with various hearing  
509 profiles. The difference between the PLV effects on speech perception in noise and in quiet is  
510 likely due to the heightened importance of temporal cues for speech perception in noise (Nie et  
511 al. 2006), and the lack of neural synchrony is associated with poor performance in  
512 psychophysical tasks requiring fine temporal perception (Zeng et al. 2005). The current results

513 can also provide validation for using the eCAP-derived PLV as a measure of neural synchrony in  
514 adult CI users (He et al. 2024). Future studies could measure neural synchrony of the CN in  
515 implanted deafened animals using both the eCAP-derived PLV and traditional single-neuron  
516 recording methods (e.g., Seki & Eggermont 2003) to further evaluate the validity of using the  
517 PLV as an index for neural synchrony of the CN.

518

### 519 **Lack of significant associations between the $IPGE_{slope}$ and Speech Perception**

520 The lack of significant associations between the  $IPGE_{slope}$  and speech perception in quiet  
521 does not support our hypothesis on the contribution of neural survival to speech perception and is  
522 not consistent with the observations in a recent study by Zamaninezhad et al. (2023). This  
523 discrepancy could be due to some critical differences between the testing materials and methods  
524 used in the two studies. The German matrix sentences in Zamaninezhad et al. (2023) consisted of  
525 syntactically correct but semantically unpredictable sentences, while the AzBio corpus consisted  
526 of meaningful sentences on everyday topics; the Freiburg monosyllable test in Zamaninezhad et  
527 al. (2023) required the listeners to repeat a single word at a time, while the AzBio test required  
528 them to repeat a full sentence in each trial. These differences allow the AzBio sentence test to  
529 better simulate real-life listening situations, but also leave room for the effect of cognitive factors  
530 such as working memory (Ingvalson et al. 2015) to modulate the speech perception performance  
531 on top of CN health condition. Therefore, it is possible that the association between the  $IPGE_{slope}$   
532 and speech perception, if any, has been eclipsed by the individual differences in cognitive factors  
533 in the present study. Future research could test both cognitive abilities and the  $IPGE_{slope}$  in the  
534 same group of CI users to evaluate their relative contributions to speech perception.

535 In addition, the  $IPGE_{slope}$  values in Zamaninezhad et al. (2023) were calculated as the  
536 difference between the AGF slopes measured with IPGs of 30  $\mu$ s and 2.1  $\mu$ s, but the present  
537 study used the AGF slopes between 42  $\mu$ s and 7  $\mu$ s for the same calculation. It is possible that  
538 the sensitivity of the  $IPGE_{slope}$  as an index of CN survival varies with the IPG levels used for  
539 eCAP recordings, and further investigation is warranted for optimizing the parameters in the  
540  $IPGE_{slope}$  measurement for the purpose of representing CN health condition.

541

## 542 **Frequency Importance Function in Speech Perception Measures**

543 While not a central focus of the present study, in the models evaluating the contributing  
544 factors to AzBio scores, we calculated the values of the  $IPGE_{slope}$  and the PLV as both  
545 unweighted averages across the tested CI electrodes and weighted averages based on the AzBio  
546 FIF. The results were similar regardless of whether the AzBio FIF weights were applied, which  
547 seemingly contradicts the definition of the FIF (Lee & Mendel 2017). A possible explanation is  
548 that the FIF used in the current study was measured in NH listeners (Lee & Mendel 2017), and  
549 thus may not be fully generalizable to CI users due to the differences in the weighting of  
550 frequency bands in speech perception between CI users and NH listeners (Sladen & Ricketts  
551 2015) and potentially larger individual differences in CI users than NH listeners (Mehr et al.  
552 2001; Bosen & Chatterjee 2016). Furthermore, the weights of adjacent frequencies could differ  
553 considerably in some FIFs (Healy et al. 2013), so that estimating the weights of CI electrodes  
554 based on a smooth curve fitted to discrete values of the empirically measured AzBio FIF may  
555 have limited validity, even if the overall FIF shape of CI users is similar to that of NH listeners.  
556 Future research could develop and validate methods for measuring the FIF in CI users and test

557 whether weighting eCAP-derived indices by the CI-based FIF can improve their capability to  
558 predict speech perception.

559

### 560 **Potential Study Limitations**

561 One potential limitation of the present study is that only 24 post-lingually deafened adult  
562 participants with generally good speech perception outcomes were included in the study.

563 Therefore, the variance in speech perception scores explained by the PLV or the  $IPGE_{slope}$  may  
564 not represent the variance explained in the entire CI patient population. Further studies in CI  
565 users with varied speech perception outcomes are warranted to assess the generalizability of the  
566 current observations. Another potential limitation of the study is that speech perception was  
567 measured only using AzBio sentences, which have high ecological validity but prone to the  
568 effects of central auditory processing and cognitive factors. In this study, only one ear was tested  
569 for each participant, including those who are bilateral CI users. Therefore, in the current dataset,  
570 it is not possible to control for potential individual differences in central auditory processing and  
571 cognitive abilities using within-participant between-ear comparisons. Future research can test  
572 both ears of bilateral CI users and/or add measurements for central auditory processing and  
573 cognitive abilities to pinpoint the crucial factors contributing to speech perception in adult CI  
574 users. Finally, the 10-talker babble was used as the competing background noise to assess speech  
575 perception performance. It does not fully capture the challenge of understanding speech in more  
576 complex environments.

577

578

## CONCLUSIONS

579

The  $IPGE_{slope}$  and the PLV are two eCAP-derived, independent indices for CN health.

580

The significant positive associations between the PLV and AzBio scores measured in noise

581

suggest that neural synchrony is important for speech perception in noise. The lack of association

582

between age and the PLV indicates that reduced neural synchrony of the CN is not the primary

583

factor accounting for the additional speech perception deficits in noise observed in elderly CI

584

users as compared to their younger counterparts. Future studies can investigate the contribution

585

of cognitive factors to speech perception and how they interact with the effects of CN health

586

status, as well as use animal models or computational modeling techniques to better understand

587

the biological underpinnings of the  $IPGE_{slope}$  and the PLV.

588 **REFERENCES**

- 589 Bates, D., Mächler, M., Bolker, B., et al. (2015). Fitting linear mixed-effects models using lme4.  
590 *J. Stat. Softw.*, 67. Available at: <http://www.jstatsoft.org/v67/i01/> [Accessed July 24,  
591 2024].
- 592 Bosen, A.K., Chatterjee, M. (2016). Band importance functions of listeners with cochlear  
593 implants using clinical maps. *J. Acoust. Soc. Am.*, 140, 3718–3727.
- 594 Brochier, T., McKay, C.M., Carlyon, R.P. (2021). Interpreting the effect of stimulus parameters  
595 on the electrically evoked compound action potential and on neural health estimates. *J.*  
596 *Assoc. Res. Otolaryngol.*, 22, 81–94.
- 597 Brown, C.J., Abbas, P.J., Gantz, B. (1990). Electrically evoked whole-nerve action potentials:  
598 Data from human cochlear implant users. *J. Acoust. Soc. Am.*, 88, 1385–1391.
- 599 Delorme, A., Makeig, S. (2004). EEGLAB: an open source toolbox for analysis of single-trial  
600 EEG dynamics including independent component analysis. *J. Neurosci. Methods*, 134, 9–  
601 21.
- 602 Dong, Y., Briaire, J.J., Biesheuvel, J.D., et al. (2020). Unravelling the temporal properties of  
603 human eCAPs through an iterative deconvolution model. *Hear. Res.*, 395, 108037.
- 604 Dong, Y., Briaire, J.J., Stronks, H.C., et al. (2023). Speech perception performance in cochlear  
605 implant recipients correlates to the number and synchrony of excited auditory nerve  
606 fibers derived from electrically evoked compound action potentials. *Ear Hear.*, 44, 276–  
607 286.
- 608 Harris, K.C., Ahlstrom, J.B., Dias, J.W., et al. (2021). Neural presbycusis in humans inferred  
609 from age-related differences in auditory nerve function and structure. *J. Neurosci.*, 41,  
610 10293–10304.

- 611 He, S., Shahsavarani, B.S., McFayden, T.C., et al. (2018). Responsiveness of the electrically  
612 stimulated cochlear nerve in children with cochlear nerve deficiency. *Ear Hear.*, 39, 238–  
613 250.
- 614 He, S., Skidmore, J., Bruce, I.C., et al. (2024). Peripheral neural synchrony in postlingually  
615 deafened adult cochlear implant users. *Ear Hear.* Available at:  
616 <https://journals.lww.com/10.1097/AUD.0000000000001502> [Accessed May 14, 2024].
- 617 He, S., Teagle, H.F.B., Buchman, C.A. (2017). The electrically evoked compound action  
618 potential: From laboratory to clinic. *Front. Neurosci.*, 11, 339.
- 619 He, S., Yuan, Y., Skidmore, J. (2023). Relationships between the auditory nerve’s ability to  
620 recover from neural adaptation, cortical encoding of and perceptual sensitivity to within-  
621 channel temporal gaps in postlingually deafened adult cochlear implant users. *Ear Hear.*,  
622 44, 1202–1211.
- 623 Healy, E.W., Yoho, S.E., Apoux, F. (2013). Band importance for sentences and words  
624 reexamined. *J. Acoust. Soc. Am.*, 133, 463–473.
- 625 Heshmat, A., Sajedi, S., Johnson Chacko, L., et al. (2020). Dendritic degeneration of human  
626 auditory nerve fibers and its impact on the spiking pattern under regular conditions and  
627 during cochlear implant stimulation. *Front. Neurosci.*, 14, 599868.
- 628 Huang, Q., Tang, J. (2010). Age-related hearing loss or presbycusis. *Eur. Arch.*  
629 *Otorhinolaryngol.*, 267, 1179–1191.
- 630 Hughes, M.L., Castioni, E.E., Goehring, J.L., et al. (2012). Temporal response properties of the  
631 auditory nerve: Data from human cochlear-implant recipients. *Hear. Res.*, 285, 46–57.
- 632 Ingvalson, E.M., Dhar, S., Wong, P.C.M., et al. (2015). Working memory training to improve  
633 speech perception in noise across languages. *J. Acoust. Soc. Am.*, 137, 3477–3486.



- 634 Jahn, K.N., Arenberg, J.G. (2020). Electrophysiological estimates of the electrode–neuron  
635 interface differ between younger and older listeners with cochlear implants. *Ear Hear.*,  
636 41, 948–960.
- 637 JASP Team (2024). JASP. Available at: <https://jasp-stats.org>.
- 638 Javel, E., Shepherd, R.K. (2000). Electrical stimulation of the auditory nerve: III. Response  
639 initiation sites and temporal fine structure. *Hear. Res.*, 140, 45–76.
- 640 Kim, J.H., Renden, R., Von Gersdorff, H. (2013). Dysmyelination of auditory afferent axons  
641 increases the jitter of action potential timing during high-frequency firing. *J. Neurosci.*,  
642 33, 9402–9407.
- 643 Kraus, N., Bradlow, A.R., Cheatham, M.A., et al. (2000). Consequences of neural asynchrony: A  
644 case of auditory neuropathy. *J. Assoc. Res. Otolaryngol.*, 1, 33–45.
- 645 Kuznetsova, A., Brockhoff, P.B., Christensen, R.H.B. (2017). lmerTest package: Tests in linear  
646 mixed effects models. *J. Stat. Softw.*, 82. Available at: <http://www.jstatsoft.org/v82/i13/>  
647 [Accessed July 24, 2024].
- 648 Leake, P.A., Hradek, G.T. (1988). Cochlear pathology of long term neomycin induced deafness  
649 in cats. *Hear. Res.*, 33, 11–33.
- 650 Lee, S., Mendel, L.L. (2017). Derivation of frequency importance functions for the AzBio  
651 sentences. *J. Acoust. Soc. Am.*, 142, 3416–3427.
- 652 Lenth, R.V. (2024). emmeans: Estimated marginal means, aka least-squares means. Available at:  
653 <https://cran.r-project.org/web/packages/emmeans/index.html>.
- 654 McKay, C.M., Smale, N. (2017). The relation between ECAP measurements and the effect of  
655 rate on behavioral thresholds in cochlear implant users. *Hear. Res.*, 346, 62–70.

- 656 Mehr, M.A., Turner, C.W., Parkinson, A. (2001). Channel weights for speech recognition in  
657 cochlear implant users. *J. Acoust. Soc. Am.*, 109, 359–366.
- 658 Nadol, J. (1997). Patterns of neural degeneration in the human cochlea and auditory nerve:  
659 Implications for cochlear implantation. *Otolaryngol. Head Neck Surg.*, 117, 220–228.
- 660 Nasreddine, Z.S., Phillips, N.A., Bédirian, V., et al. (2005). The Montreal Cognitive Assessment,  
661 MoCA: A brief screening tool for mild cognitive impairment. *J. Am. Geriatr. Soc.*, 53,  
662 695–699.
- 663 Nie, K., Barco, A., Zeng, F.-G. (2006). Spectral and temporal cues in cochlear implant speech  
664 perception. *Ear Hear.*, 27, 208–217.
- 665 Pfungst, B.E., Hughes, A.P., Colesa, D.J., et al. (2015). Insertion trauma and recovery of function  
666 after cochlear implantation: Evidence from objective functional measures. *Hear. Res.*,  
667 330, 98–105.
- 668 Prado-Guitierrez, P., Fewster, L.M., Heasman, J.M., et al. (2006). Effect of interphase gap and  
669 pulse duration on electrically evoked potentials is correlated with auditory nerve survival.  
670 *Hear. Res.*, 215, 47–55.
- 671 R Core Team (2024). R: A language and environment for statistical computing. Available at:  
672 <https://www.R-project.org/>.
- 673 Ramekers, D., Versnel, H., Strahl, S.B., et al. (2014). Auditory-nerve responses to varied inter-  
674 phase gap and phase duration of the electric pulse stimulus as predictors for neuronal  
675 degeneration. *J. Assoc. Res. Otolaryngol.*, 15, 187–202.
- 676 Rask-Andersen, H., Liu, W., Linthicum, F. (2010). Ganglion cell and ‘dendrite’ populations in  
677 electric acoustic stimulation ears. In P. Van De Heyning & A. Kleine Punte, eds.

- 678 *Advances in Oto-Rhino-Laryngology*. (pp. 14–27). S. Karger AG. Available at:  
679 <https://pubmed.ncbi.nlm.nih.gov/19955718/> [Accessed October 23, 2024].
- 680 Resnick, J.M., O’Brien, G.E., Rubinstein, J.T. (2018). Simulated auditory nerve axon  
681 demyelination alters sensitivity and response timing to extracellular stimulation. *Hear.*  
682 *Res.*, 361, 121–137.
- 683 Roberts, D.S., Lin, H.W., Herrmann, B.S., et al. (2013). Differential cochlear implant outcomes  
684 in older adults. *The Laryngoscope*, 123, 1952–1956.
- 685 Rumschlag, J.A., McClaskey, C.M., Dias, J.W., et al. (2022). Age-related central gain with  
686 degraded neural synchrony in the auditory brainstem of mice and humans. *Neurobiol.*  
687 *Aging*, 115, 50–59.
- 688 Schwartz-Leyzac, K.C., Colesa, D.J., Buswinka, C.J., et al. (2019). Changes over time in the  
689 electrically evoked compound action potential (ECAP) interphase gap (IPG) effect  
690 following cochlear implantation in Guinea pigs. *Hear. Res.*, 383, 107809.
- 691 Schwartz-Leyzac, K.C., Pfungst, B.E. (2018). Assessing the relationship between the electrically  
692 evoked compound action potential and speech recognition abilities in bilateral cochlear  
693 implant recipients. *Ear Hear.*, 39, 344–358.
- 694 Seki, S., Eggermont, J.J. (2003). Changes in spontaneous firing rate and neural synchrony in cat  
695 primary auditory cortex after localized tone-induced hearing loss. *Hear. Res.*, 180, 28–38.
- 696 Seyyedi, M., Viana, L.M., Nadol, J.B. (2014). Within-subject comparison of word recognition  
697 and spiral ganglion cell count in bilateral cochlear implant recipients. *Otol. Neurotol.*, 35,  
698 1446–1450.

- 699 Skidmore, J., Ramekers, D., Colesa, D.J., et al. (2022). A broadly applicable method for  
700 characterizing the slope of the electrically evoked compound action potential amplitude  
701 growth function. *Ear Hear.*, 43, 150–164.
- 702 Sladen, D.P., Ricketts, Todd.A. (2015). Frequency importance functions in quiet and noise for  
703 adults with cochlear implants. *Am. J. Audiol.*, 24, 477–486.
- 704 Sladen, D.P., Zappler, A. (2015). Older and younger adult cochlear implant users: speech  
705 recognition in quiet and noise, quality of life, and music perception. *Am. J. Audiol.*, 24,  
706 31–39.
- 707 Spahr, A.J., Dorman, M.F., Litvak, L.M., et al. (2012). Development and validation of the AzBio  
708 sentence lists. *Ear Hear.*, 33, 112–117.
- 709 Starr, A., Zeng, F.G., Michalewski, H.J., et al. (2008). Perspectives on auditory neuropathy:  
710 disorders of inner hair cell, auditory nerve, and their synapse. In *The Senses: A*  
711 *Comprehensive Reference*. (pp. 397–412). Elsevier. Available at:  
712 <https://linkinghub.elsevier.com/retrieve/pii/B9780123708809000335> [Accessed  
713 September 12, 2024].
- 714 Takanen, M., Strahl, S., Schwarz, K. (2024). Insights into electrophysiological metrics of  
715 cochlear health in cochlear implant users using a computational model. *J. Assoc. Res.*  
716 *Otolaryngol.* Available at: <https://link.springer.com/10.1007/s10162-023-00924-z>  
717 [Accessed September 12, 2024].
- 718 Tejani, V.D., Abbas, P.J., Brown, C.J. (2017). Relationship between peripheral and  
719 psychophysical measures of amplitude modulation detection in cochlear implant users.  
720 *Ear Hear.*, 38, e268–e284.

- 721 Won, J.H., Humphrey, E.L., Yeager, K.R., et al. (2014). Relationship among the physiologic  
722 channel interactions, spectral-ripple discrimination, and vowel identification in cochlear  
723 implant users. *J. Acoust. Soc. Am.*, 136, 2714–2725.
- 724 Wu, P., O’Malley, J.T., De Gruttola, V., et al. (2020). Age-related hearing loss is dominated by  
725 damage to inner ear sensory cells, not the cellular battery that powers them. *J. Neurosci.*,  
726 40, 6357–6366.
- 727 Wu, P., O’Malley, J.T., Liberman, M.C. (2023). Neural degeneration in normal-aging human  
728 cochleas: Machine-learning counts and 3D mapping in archival sections. *J. Assoc. Res.*  
729 *Otolaryngol.*, 24, 499–511.
- 730 Wu, P.Z., Liberman, L.D., Bennett, K., et al. (2019). Primary neural degeneration in the human  
731 cochlea: Evidence for hidden hearing loss in the aging ear. *Neuroscience*, 407, 8–20.
- 732 Wu, P.-Z., O’Malley, J.T., De Gruttola, V., et al. (2021). Primary neural degeneration in noise-  
733 exposed human cochleas: Correlations with outer hair cell loss and word-discrimination  
734 scores. *J. Neurosci.*, 41, 4439–4447.
- 735 Xie, Z., Gaskins, C.R., Shader, M.J., et al. (2019). Age-related temporal processing deficits in  
736 word segments in adult cochlear-implant users. *Trends Hear.*, 23, 2331216519886688.
- 737 Xing, Y., Samuvel, D.J., Stevens, S.M., et al. (2012). Age-related changes of myelin basic  
738 protein in mouse and human auditory nerve O. Bermingham-McDonogh, ed. *PLoS ONE*,  
739 7, e34500.
- 740 Yuan, Y., Skidmore, J., He, S. (2022). Interpreting the interphase gap effect on the electrically  
741 evoked compound action potential. *JASA Express Lett.*, 2, 027201.

- 742 Zaltz, Y., Buganim, Y., Zechoval, D., et al. (2020). Listening in noise remains a significant  
743 challenge for cochlear implant users: evidence from early deafened and those with  
744 progressive hearing loss compared to peers with normal hearing. *J. Clin. Med.*, 9, 1381.
- 745 Zamaninezhad, L., Mert, B., Benav, H., et al. (2023). Factors influencing the relationship  
746 between cochlear health measures and speech recognition in cochlear implant users.  
747 *Front. Integr. Neurosci.*, 17, 1125712.
- 748 Zanin, J., Rance, G. (2024). Objective determination of site-of-lesion in auditory neuropathy.  
749 *Ear Hear.* Available at: <https://journals.lww.com/10.1097/AUD.0000000000001589>  
750 [Accessed September 30, 2024].
- 751 Zeng, F.-G. (2004). Trends in cochlear implants. *Trends Amplif.*, 8, 1–34.
- 752 Zeng, F.-G., Kong, Y.-Y., Michalewski, H.J., et al. (2005). Perceptual consequences of disrupted  
753 auditory nerve activity. *J. Neurophysiol.*, 93, 3050–3063.
- 754